Bending and vibrations analyses of laminated beams by using a zig-zag-layer-wise theory

Bending and vibrations analyses of laminated beams by using a zig-zag-layer-wise theory

M. Filippi*, E. Carrera†

Department of Mechanical and Aerospace Engineering, Politecnico di Torino,
Corso Duca degli Abruzzi 24, 10129 Torino, Italy.

Submitted to **Composites Part B: engineering**

Author for correspondence:
M. Filippi, Research Fellow,
Department of Mechanical and Aerospace Engineering,
Politecnico di Torino,
Corso Duca degli Abruzzi 24,
10129 Torino, Italy,
e-mail: matteo.filippi@polito.it

*Research Fellow, e-mail: matteo.filippi@polito.it
†Professor of Aerospace Structures and Aeroelasticity, e-mail: erasmo.carrera@polito.it

Abstract

This paper proposes one-dimensional layer-wise theories that make use of higher-order zig-zag functions defined over fictitious/mathematical layers of the cross-sectional area. These advanced kinematics enable the computational costs to be reduced while the accuracy of the classical layer-wise theories in which the number of physical and numerical layers coincide, is maintained. Variable kinematics theories have been obtained using piecewise continuous power series expansions of an arbitrary order defined over the whole cross-section of the structure. As in the classical layer-wise approach, the cross-section can be divided into a variable number of mathematical subdomains. The expansion order of each subdomain is therefore an input parameter of the analysis. This feature enables the solution to be refined locally as the kinematics expansion can be enriched over generic regions of the cross-section. The governing equations have been obtained by applying the Principle of Virtual Displacements, along with the Carrera Unified Formulation, and have been solved using the Finite Element method. Numerical simulations have been performed considering laminated and sandwich beams with very low length-to-depth ratio values. Comparisons between the present results and solutions available in the literature have pointed out the advantages of this approach, in terms of accuracy of the displacements, of the stress distributions over the beam cross-section and of the natural frequencies with respect to the classical layer-wise theories.

Keywords: B. Laminates; B. Layered structures; C. Finite element analysis (FEA); C. Numerical Analysis; Zig-zag-layer-wise theory

1 Introduction

The fulfillment of the more and more restrictive requirements in vehicles design has led to the extensive use of composite materials. This fact can be corroborated by considering the significant efforts that have been made by the most influential industries to develop new commercial airplanes with the highest possible percentage of advanced materials (more than 50%). The current tendency is to further augment this percentage. Unfortunately, despite their recognized advantages, composite structures exhibit much more complex mechanical behavior than their metallic counterparts. For this reason, a huge number of numerical simulations, supported by expensive test campaigns, is required to ensure the fulfillment of the safety requirements. Therefore, the development of reliable and computationally effective tools for the description of the mechanical response of composites is still of practical importance. Over the years, either one- or two-dimensional structural theories have frequently been used to solve the 3D elasticity problem. Well-known classical theories, namely the Euler-Bernoulli [1] and Timoshenko [2] beam models and the corresponding Love-Kirchhoff [3] and Reissner-Mindlin [4] plate approaches, are not able to provide an accurate description of the stress state of layered structures. The main drawbacks are derived from the adopted linear displacement assumption through the thickness, which cannot intrinsically satisfy the interlaminar shear stress continuity and the surface conditions prescribed by the equilibrium equations. Thus, advanced formulations, based on the equivalent single layer (ESL) and layer-wise (LW) approaches, have been conceived to overcome these issues. According to the former method, the number of problem unknowns does not depend on the number of plies, contrary to what happens with the LW technique. Within the ESL context, the fulfilment of the governing equations is pursued by increasing the order of the interpolating expansions of the displacement components. Early attempts were proposed in [5, 6] and [7, 8], where quadratic and cubic power series expansions were developed, respectively. It was demonstrated that these displacement models can be obtained directly from Reddy's third-order shear deformation theory [9], as particular cases. In order to correctly predict the "local" responses of laminated structures, Matsunaga considered the displacement components as expansions of arbitrary orders based on truncated power series expansions of the z-coordinate [10]. Axial stress distributions were obtained from Hooke's law, whereas the shear stress profiles were computed by integrating the equilibrium equations. Other ESL shear deformation theories that exploit the properties of non-polynomial functions have been proposed, such as [11, 12] and [13]. Although the improvements introduced by these advanced models are certainly significant, they provide continuous strain distributions through the lamination direction. This feature leads to interlaminar discontinuity of the shear stresses. Therefore, piecewise continuous displacement fields have been developed with the aim of reproducing the typical zig-zag displacement profiles. These formulations have been derived in the frameworks of ESL [14, 15, 16] and LW [17] approaches, using either displacement-based [18] or mixed [19] variational statements. A detailed description of zig-zag theories, especially those obtained in the ESL context, can be found in [20]. ESL

zig-zag theories are able to combine a high level of accuracy with a low computational cost. However, their derivation often represents a complex task since it requires a number of assumptions related to the laminate properties (degree of anisotropy, thickness ratios etc.). Despite the higher computational cost, compared to ESL models, the LW description is probably the most reliable and general approach for the study of layered structures. According to this methodology, each cross-sectional subdomain can be treated either as a mathematical or a physical layer, in which the displacement components are arbitrarily expanded. The kinematic expansion within each subdomain must ensure the continuity of the displacements through the interfaces. To this end, polynomial [21, 22] as well as trigonometric [23, 24] functions have been used. Moreover, the assembly technique at the interface level enables the study of delamination phenomena to be performed [25, 26] and [27]. Recently, both ESL and LW theories have successfully been developed by means of the Carrera Unified Formulation (CUF) for the analyses of laminated structures [28]. As far as the ESL theories are concerned, the authors (Carrera and Filippi) provided comparisons of several kinematic models, obtained with arbitrary functions of the cross-sectional coordinates [29, 30]. The Murakami zig-zag function (hereafter referred to as 'MZZ') was added to the displacement fields in order to fulfill the C_z^0-requirement. The same formulations were subsequently adopted for stress [31] and dynamic [32] analyses of functionally graded structures. On the other hand, the CUF-LW models were derived using Lagrange [33, 34] and Legendre-type [35] expansions, which enabled compact and thin-walled layered structures to be analyzed. Another interesting LW formulation, in which the multi-line refined beam models were developed, was proposed by Carrera and Pagani [36]. According to this approach, subdomain kinematics was approximated using Taylor-like expansions, by locally imposing displacement continuity by means of Lagrange's multipliers. A similar approach was used by Yang *et al.* for the analysis of wrinkling in stiff thin films, which rest on compliant thick elastic substrates [37]. As far as plate theories are concerned, mixed ESL/LW models have recently been proposed for the static [38, 39] and nonlinear vibration analyses [40] of layered structures. These models exploit the interesting characteristics of the Legendre polynomials in order to obtain variable kinematic theories through the plate thickness. ESL-LW models were derived using both displacement-based and mixed variational statements. The present paper has the aim of presenting a new class of refined beam displacement-based theories that can provide both ESL and LW kinematic descriptions. The displacement components have been written as power series of piecewise continuous functions of arbitrary orders. Since these functions are defined over the whole cross-section, the expansion order of each subdomain becomes an input parameter of the analysis. Therefore, the kinematics theory can be locally enriched while the displacement continuity through the interfaces is preserved. The equations of motion have been derived from the Principle of Virtual Displacements (PVD) and solved through a classical 1D finite element technique. The numerical applications have demonstrated the accuracy of the proposed theories, in terms of displacements, stress distributions and natural frequencies, with respect

to the results available in the literature.

2 Equations of motion in CUF form

The general form of the PVD establishes the well-known relation between the kinematically admissible perturbations (indicated by δ) of the strain energy (L_{int}), inertial energy (L_{ine}) and the external work (L_{ext}) exerted by the forces ($\tilde{\boldsymbol{F}}$):

$$\delta L_{int} = \delta L_{ext} + \delta L_{ine} \tag{1}$$

The energies of Eq. 1 are expressed in terms of the displacement vector, $\boldsymbol{u}^T = [u_x, u_y, u_z]$, as it follows

$$\int_V \delta \boldsymbol{u}^T \boldsymbol{D}^T \boldsymbol{C} \boldsymbol{D} \boldsymbol{u} \, dV = \int_V \delta \boldsymbol{u}^T \tilde{\boldsymbol{F}} \, dV + \int_V \delta \boldsymbol{u}^T \rho \ddot{\boldsymbol{u}} \, dV \tag{2}$$

where the differential operator $\boldsymbol{D}$ is a matrix that defines the strain-displacement relations, $\boldsymbol{C}$ is the stiffness matrix of the Hooke's law, ρ is the material density, and $\ddot{\boldsymbol{u}}$ is the acceleration vector.
CUF is a simple methodology, which essentially offers two main advantages:

1. the governing equations are systematically obtained from Eq. 2 regardless of the adopted kinematic assumptions;

2. comparisons between different kinematic theories can be easily performed to identify which are the most effective solutions depending on the problem characteristics.

The fundamental CUF equation is based on a simple separation of variables, according to which, the 3D displacement field $\boldsymbol{u}(x, y, z, t)$ is being assumed to be a combination of products of cross-sectional functions F_τ(x,z) and the generalized displacement vector $\boldsymbol{u}_\tau$(y,t)

$$\boldsymbol{u}(x, y, z, t) = F_\tau(x, z)\boldsymbol{u}_\tau(y, t) \qquad \tau = 1, 2, \ldots, N \tag{3}$$

The subscript τ stands for summation, and N is the number of terms in the expansion. In this work, the F_τ(x,z) functions are assumed $a - priori$, and the generalized displacement vector along the beam axis is interpolated through a classical finite element technique

$$\mathbf{u}_\tau(y, t) = N_i(y)\mathbf{q}_{\tau i}(t) \tag{4}$$

where $\mathbf{q}_{\tau i}^T(t) = [q_{u_{x_{\tau i}}}, q_{u_{y_{\tau i}}}, q_{u_{z_{\tau i}}}]$ is the nodal displacement vector, and N_i are the lagrangian shape functions along the longitudinal axis (see [41] (§5.2.2)). The linear strain-displacement relations and the Hooke's law are

$$\boldsymbol{\epsilon} = \boldsymbol{D}\,\boldsymbol{u} \qquad \boldsymbol{\sigma} = \boldsymbol{C}\,\boldsymbol{\epsilon} \tag{5}$$

The expressions of the stiffness coefficients of $\boldsymbol{C}$ matrix and the differential mathematical operator, $\boldsymbol{D}$, can be found in [42]. To obtain the variational statement in CUF form, Eqs. 3, 4 and 5 are substituted in Eq. 2

$$\delta \boldsymbol{q}_{\tau i}^T \int_V F_\tau N_i \boldsymbol{D}^T \boldsymbol{C} \boldsymbol{D} F_s N_j \, dV \, \boldsymbol{q}_{sj} \;=\; \delta \boldsymbol{q}_{\tau i}^T \int_V F_\tau N_i \, \tilde{\boldsymbol{F}} \, dV + \delta \boldsymbol{q}_{\tau i}^T \int_V F_\tau N_i \boldsymbol{I} \rho F_s N_j \, dV \, \ddot{\boldsymbol{q}}_{sj} \tag{6}$$

where $\boldsymbol{I}$ is the 3-by-3 identity matrix. The variational principle of Eq. 6 is satisfied for all possible perturbations if the following equations of motion are fulfilled

- static problem:

$$\boldsymbol{K}^{ij\tau s} \boldsymbol{q}_{sj} = \boldsymbol{P} \tag{7}$$

- undamped homogenous dynamic problem:

$$\boldsymbol{M}^{ij\tau s} \ddot{\boldsymbol{q}}_{sj} + \boldsymbol{K}^{ij\tau s} \boldsymbol{q}_{sj} = 0 \tag{8}$$

It is straightforward to demonstrate that for given indexes, the systems of Eqs. 7 and 8 consist of three equations related to the three displacement components. Indeed, the dimension of both stiffness $\boldsymbol{K}^{ij\tau s}$ and mass $\boldsymbol{M}^{ij\tau s}$ matrices is 3-by-3, while the loading vector $\boldsymbol{P}$ is a 3-by-1 vector. Furthermore, neither the nature of functions F_τ nor their number N modifies the expressions of these mathematical operators, which are traditionally called *fundamental nuclei*. The explicit expressions of the *fundamental nuclei* can be found in [43]. The complete structural matrices related to the adopted mathematical model are being obtained through the assembly technique schematically shown in Fig. 1.

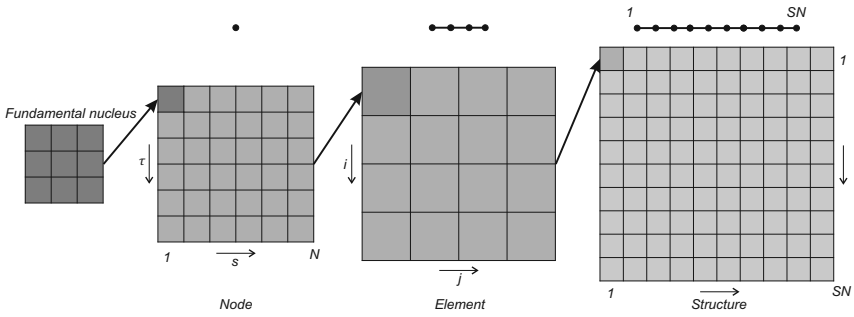

Figure 1: Graphical representation of the assembly procedure.

3 Layerwise models with higher-order zig-zag functions

Let us consider a laminated structure with a prismatic cross-section constituted of n layers. The cross-section can be considered divided into K subdomains, which can include one or more layers, having the thickness and width equal to $h_k = z_{k-1} - z_k$ and b, respectively (see Fig. 2).

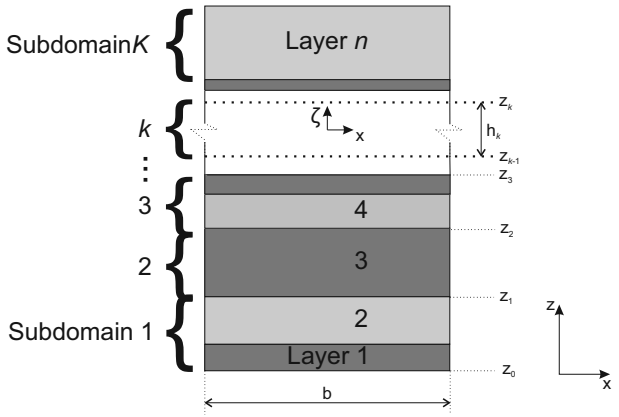

Figure 2: Cross-section of a laminated structure.

The variable kinematic field is written by using an arbitrary number of continuous piecewise polynomial functions, which are defined over the entire cross-section. The p_k-order polynomial expansion of generic subdomain 'k' is a combination of power functions of the cross-sectional coordinates, 'x' and 'z'. Assuming that the mechanical properties vary discretely along the thickness direction, the F_τ functions defined over the k-th subdomain are

$$F_\tau(x,z)_k^{(p_x,p_z)} = \begin{cases} (-1)^{p_z}\left(\frac{2\,x}{b}\right)^{p_x}, & \text{if } \mathrm{z} < \mathrm{z_{k-1}} \\ (1)\left(\frac{2\,x}{b}\right)^{p_x}\left(\frac{2\,\zeta}{h_k}\right)^{p_z}, & \text{if } \mathrm{z_{k-1}} < \mathrm{z} < \mathrm{z_k} \\ (1)^{p_z}\left(\frac{2\,x}{b}\right)^{p_x}, & \text{if } \mathrm{z} > \mathrm{z_k} \end{cases} \tag{9}$$

where the superscripts p_x, p_z are the polynomial orders and ζ is the subdomain thickness coordinate, which ranges from $-h_k/2$ to $h_k/2$. Since the polynomial orders are input parameters of the analysis, they can be arbitrarily defined for each cross-sectional subdomain. Moreover, the F_τ functions are defined such that they range from -1 and +1 regardless on the chosen (p_x, p_z) combination (see Fig. 3).

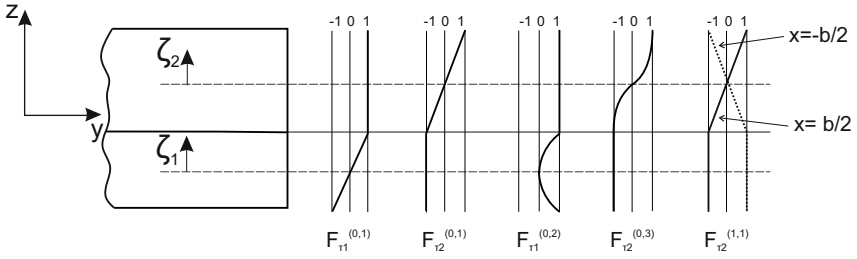

Figure 3: Various F_τ functions for a 2-subdomain beam.

It is noteworthy that, depending on the number of considered subdomains 'K', the proposed methodology can represent either an equivalent single layer approach (K=1) or a "pure" layer-wise kinematic model (K=n). Figure 4 shows the piecewise functions up to the third order for the middle region of a 3-subdomain cross-section.

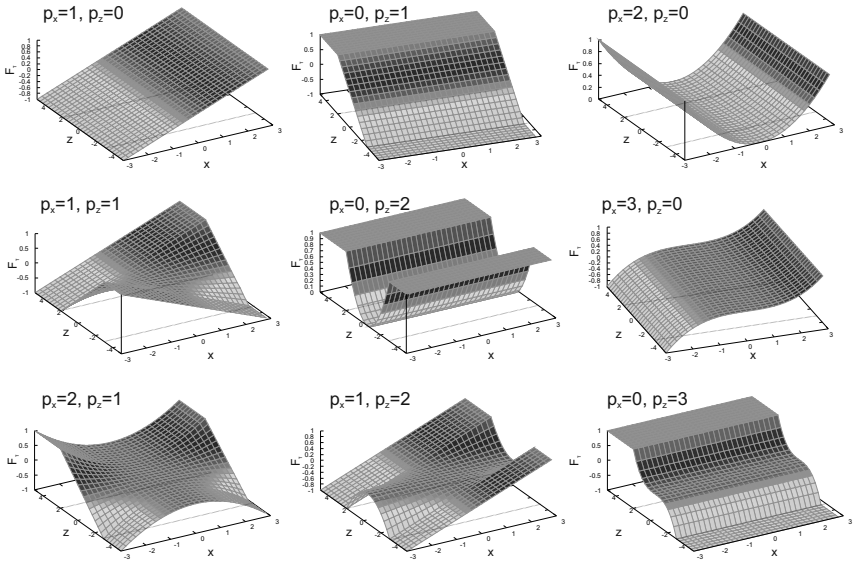

Figure 4: The F_τ functions computed on a subdomain defined between $z_{k-1} = -3$ and $z_k = 2$.

Owing to the zig-zag form of such displacement fields, first derivatives (and, therefore, the strain field) with respect to the thickness direction, $\mathrm{F}_{\tau,z}$, are discontinuous as shown in Fig. 5

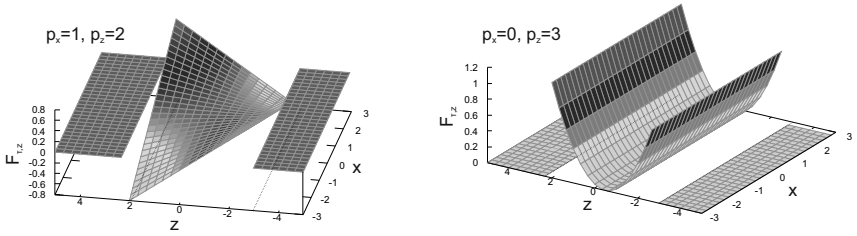

Figure 5: The $\mathrm{F}_{\tau,z}$ derivatives computed on a subdomain defined between $z_{k-1} = -3$ and $z_k = 2$.

The proposed layer-wise expansions are being denoted with the following notation

- TE-LW(p_c): the subscript 'c' indicates that the 'p'-th order expansion is used for each subdomain. If the number of subdomains does not coincide with the number of structural layers, the superscript ($\star$) is added to the notation (TE-LW(p_c)$\star$);
- TE-LW($p_1 - p_2 - \ldots - p_K$): the local expansion order of each subdomain 'p_k' is explicitly reported in brackets starting from the bottom surface.

According to this notation, two expressions of the first component of the displacement field (u_x) are reported below for a 2-subdomains structure (see Eq. 9)

- TE-LW(2_c):

$$u_x = 1\,u_{x1} + F_\tau(x,z)_1^{(1,0)}\,u_{x2} + F_\tau(x,z)_1^{(0,1)}\,u_{x3} + F_\tau(x,z)_2^{(0,1)}\,u_{x4} + F_\tau(x,z)_1^{(2,0)}\,u_{x5} + \\ + F_\tau(x,z)_1^{(1,1)}\,u_{x6} + F_\tau(x,z)_1^{(0,2)}\,u_{x7} + F_\tau(x,z)_2^{(1,1)}\,u_{x8} + F_\tau(x,z)_2^{(0,2)}\,u_{x9}$$

- TE-LW(1-2):

$$u_x = 1\,u_{x1} + F_\tau(x,z)_1^{(1,0)}\,u_{x2} + F_\tau(x,z)_1^{(0,1)}\,u_{x3} + F_\tau(x,z)_2^{(0,1)}\,u_{x4} + F_\tau(x,z)_2^{(2,0)}\,u_{x5} + \\ + F_\tau(x,z)_2^{(1,1)}\,u_{x6} + F_\tau(x,z)_2^{(0,2)}\,u_{x7}$$

where u_{x1}, u_{x2}, ..., u_{xN} are the theory unknowns. It should be observed that the functions $F_\tau(x,z)_k{}^{(p_x,0)}$ appear only once in the expansions since they coincide for all subdomains.

4 Static analysis

This section has the aim of presenting a number of results derived from bending analyses performed on laminated prismatic beams with rectangular cross-sections, which are made of orthotropic and isotropic materials. The numbers of degrees of freedom (DOFs) required for the TE-LW models have been obtained using the following formula

$$DOFs = (3 \times N) \times SN$$

where 'SN' stands for the structural beam nodes along the longitudinal axis.

4.1 8-layer laminated beam

The cantilever 8-layer laminated beam investigated in [29] has been considered. The geometry and the stacking sequence are shown in Fig. 6. All the layers have the same Young's Modulus in the transverse direction $E_2 = E_3 = 1$GPa, shear modulus $G = 0.5$ GPa and, Poisson's ratio $\nu = 0.25$, whereas the layers labeled with 1 have a longitudinal modulus $E_1 = 30$ GPa and the layers labeled with 2 have $E_1 = 5$ GPa. A concentrated load, $F_z = -0.2$ N, has been applied at the tip and ten 4-node beam elements have been used to model the structure along the longitudinal direction. The results, in terms of maximum displacement and maximum longitudinal stress at mid-span, are reported in Tab. 1 and compared with those available in the literature. The analyses have been performed using linear, quadratic and cubic Taylor-type expansions within each sub-domain. Seven and 8 sub-domains have been define in order to model the cross-section, by considering the -1.25 $\leq$ z $\leq$ 1.25 mm region to be constituted by either 1 or 2 layers, respectively. Moreover, the σ_{yy} and σ_{yz} distributions along the z axis are shown in Fig. 7,

where the present beam models are compared to the analytical solution derived by the theory of elasticity presented in [44].

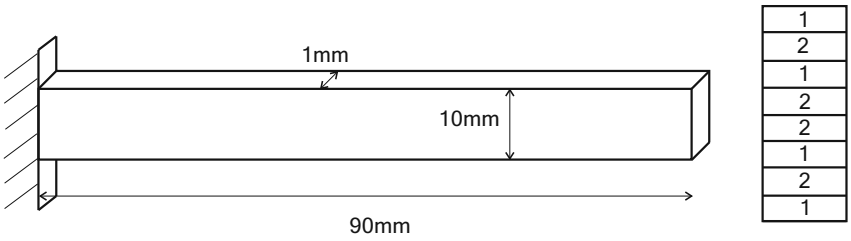

Figure 6: The 8-layer laminated beam.

	$-w \times 10^{-2}$	$-\sigma_{yy}$	DOFs
Surana and Nguyen [45]	3.031	720	-
Davalos and Barbero [46]	3.029	700	-
Lin and Zhang [47]	3.060	750	-
Vo and Thai [48]	3.024	-	-
Carrera and Pagani [36]	3.026	731	6696
Carrera *et al.* [34]	3.029	730	4743
EBBT	2.629	730	279
TBT	2.988	730	279
TE_1	2.992	730	279
TE_2	2.985	730	558
TE_3	3.032	729	930
TE_5	3.042	730	1953
TE_8	3.046	730	4185
TE-LW(1_c)	2.857	731	930
TE-LW(2_c)	3.026	731	2511
TE-LW(3_c)	3.026	731	4836
TE-LW(1_c)*	2.858	731	837
TE-LW(2_c)*	3.026	731	2232
TE-LW(3_c)*	3.026	731	4278

subscript 'c': same expansion order is used within each sub-domain.
superscript '$*$': 7 sub-domains.

Table 1: w displacement and σ_{yy} values composite cantilevered beam.

It has been observed that, at least the quadratic piece-wise expansions (TE-LW(2_c) and TE-LW(2_c)*) are required to obtain accurate estimations of the displacement and transverse shear stress distribution (see Fig. 7). The TE-LW(1_c) and TE-LW(1_c)* linear theories provided the same σ_{yy} distributions as the higher-order models.

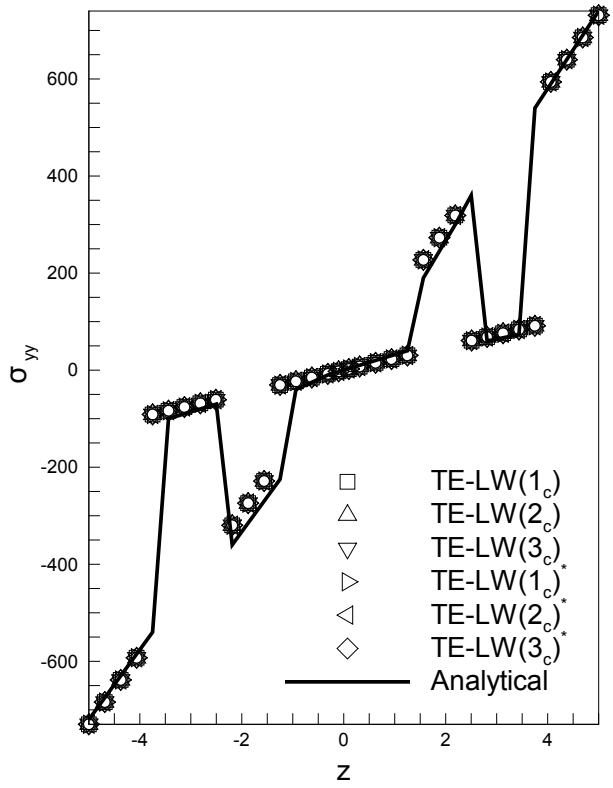

(a) σ_{yy} at y = 45 mm

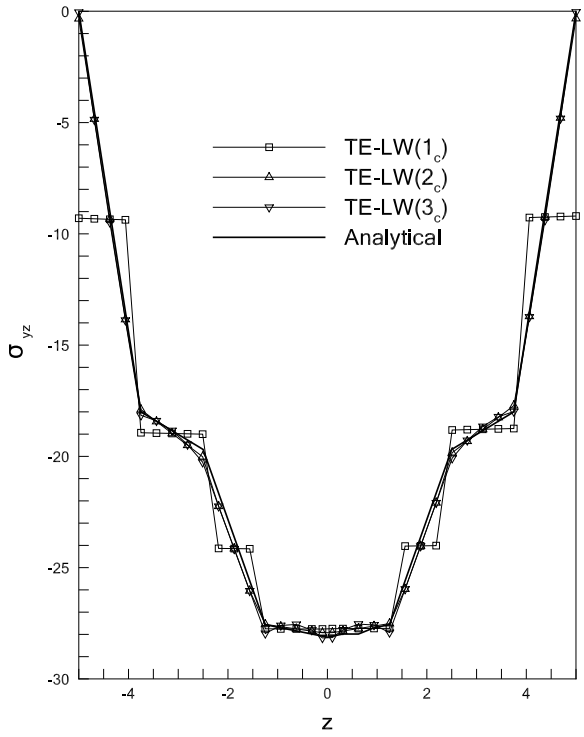

(b) σ_{yz} at y = 45 mm

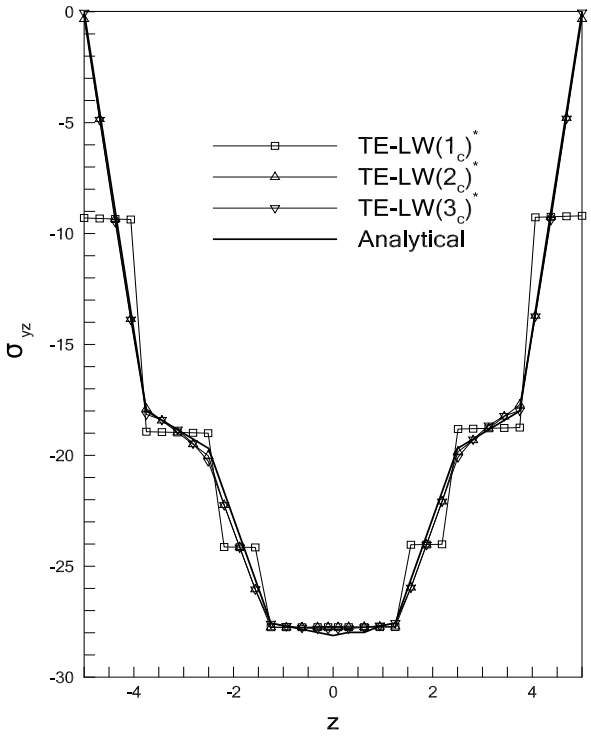

(c) σ_{yz} at y = 45 mm

Figure 7: Distribution of axial, $\sigma_y y$, and transverse shear, $\sigma_y z$, stresses for the 8-layer laminated beam.

4.2 Symmetric and antisymmetric laminated beams

Three- and 2-layer beams with square cross-sections have been studied. All the laminae have the same thickness and are made of the same orthotropic material, which has the following properties:

$$\frac{E_L}{E_T} = 25 \qquad \frac{G_{LT}}{G_{TT}} = 2.5$$
$$G_{TT} = 0.2E_T \quad \nu_{LT} = 0.1 \quad \nu_{TT} = 0.3$$

where L indicates the fiber direction and T stands for the direction normal to the fibers. The ratio between the beam length, 'L_s', and the side dimension of the cross-section, 'b', was assumed equal to 4. The results are provided in the following non-dimensional forms

$$w^* = 100\frac{E_T b h^3}{q_0 L^4} w; \quad \sigma_{ij}^* = \frac{\sigma_{ij}}{q_0} \quad \text{with} \quad i,j = x,y,z \tag{10}$$

where q_0 is the intensity of the load uniformly distributed over the face of the cantilevered beams. The symmetric [0/90/0] and antisymmetric [0/90] configurations were previously analyzed in [29] and [36], in which higher-order theories based on equivalent single-layer and multi-line approaches were adopted. The corresponding results have been taken as reference solutions and are reported in Tab. 2.

The agreements between the different kinematic theories, in terms of maximum displacement and normal transverse stress, are somewhat significant. As far as the computational cost is concerned, the proposed theory is comparable with the multi-line approach, since the number of unknowns increases as the theory order and the number of layers increases. Figure 8 shows the through-the-thickness distributions of σ_{yy} and σ_{zz} for both structures, computed with different expansions within each layer. Comparisons with converged solid FE solutions have revealed that the third-order polynomial expansion (TE-LW(3_c)) is able to provide accurate approximations of the stress profiles.

Moreover, other stress analyses have been performed considering the $[\theta_1/\theta_2/\theta_3]$ lamination sequence, where θ_1, θ_2 and θ_3 denote the fiber angles of the lower, middle and upper layers, respectively. The results, in terms of through-the-thickness distributions of the stresses and displacements, have been compared with converged FE solutions and are shown in Fig. 9.

It can be observed that the results obtained with the TE-LW(7_c) are close to the reference solutions, regardless of which stacking sequence is considered. Furthermore, it should be noted that the stress-free condition on the beam boundary surfaces is substantially fulfilled, even though, it had not been $a-priori$ imposed. As far as [30/30/45] is concerned, a refined theory would be required to reduce the interface discontinuities of the normal transverse stress σ_{zz}.

	[0/90/0]			[0/90]		
	w^*	$-\sigma_{zz}^*$	DOFs	w^*	$-\sigma_{zz}^*$	DOFs
			Carrera *et al.* [29]			
Solid	17.98	1.03	103920	43.09	1.02	198300
TE6^{Mzz}	17.84	1.03	1914	42.26	1.01	1914
TE6	17.14	0.99	1848	42.16	1.04	1848
TE3^{Mzz}	17.83	1.02	726	41.66	1.04	726
TE3	16.76	1.04	660	41.63	1.13	660
FSDT	14.02	0.00	198	40.88	0.00	198
EBBT	6.22	0.00	198	31.96	0.00	198
			Carrera and Pagani [36]			
ML2/2/2	17.69	1.01	1188	–	–	–
ML3/2/3	17.83	1.03	1716	–	–	–
ML3/3	–	–	–	42.30	–	1320
			Present			
TE-LW(1_c)	17.43	0.83	330	41.18	0.42	264
TE-LW(2_c)	17.81	1.03	792	41.68	1.03	594
TE-LW(3_c)	17.94	1.01	1452	42.61	1.07	1056
TE-LW(4_c)	17.95	1.01	2310	42.62	1.01	1650
TE-LW(5_c)	17.96	0.99	3366	42.62	0.99	2376
TE-LW(6_c)	17.96	0.98	4620	42.63	0.99	3234
TE-LW(7_c)	17.96	1.00	6072	42.63	1.00	4224

'FSDT': first-order shear deformation theory.

'EBBT': Euler-Bernoulli beam theory.

'Mzz': Murakami's zig-zag function.

'–': result not provided.

Table 2: Non-dimensional tip deflections and normal transverse stresses of the laminated beams [0/90/0] and [0/90].

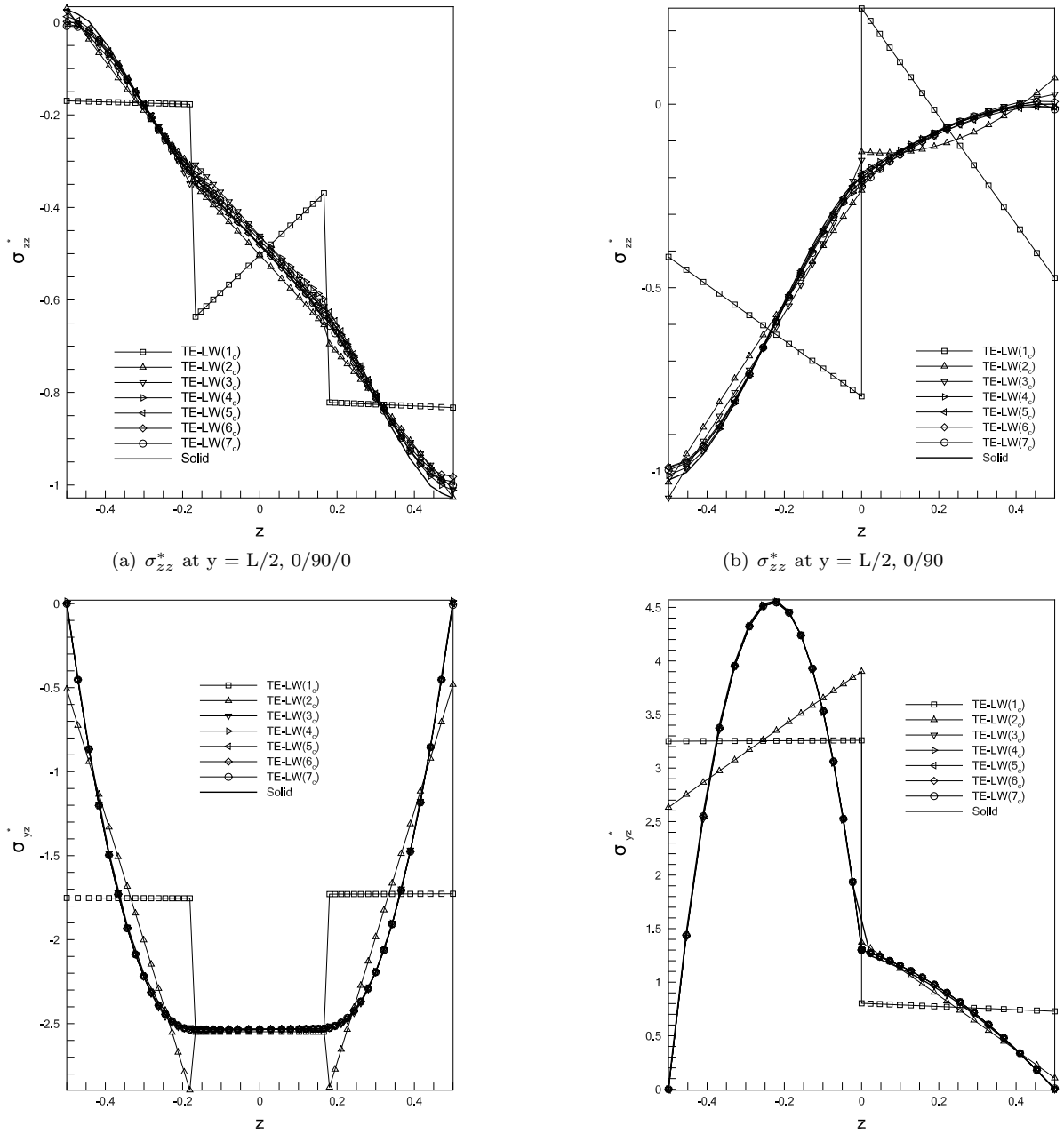

(a) σ^*_{zz} at y = L/2, 0/90/0

(b) σ^*_{zz} at y = L/2, 0/90

(c) σ^*_{yz} at y = L/2, 0/90/0

(d) σ^*_{yz} at y = L/2, 0/90

Figure 8: Through-the-thickness distributions of stresses of the 3- and 2-layer laminated beam [0/90/0], [0/90].

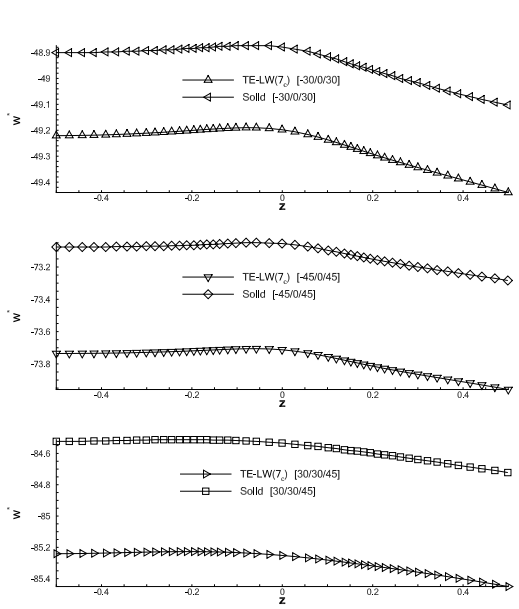

(a) w* at y = L

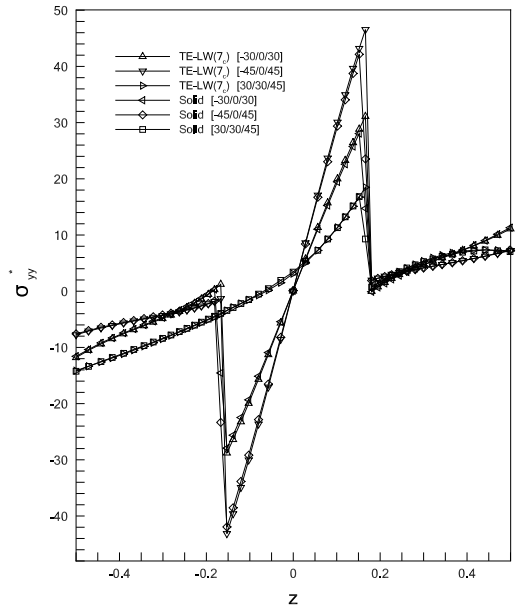

(b) σ^*_{yy} at y = L/2

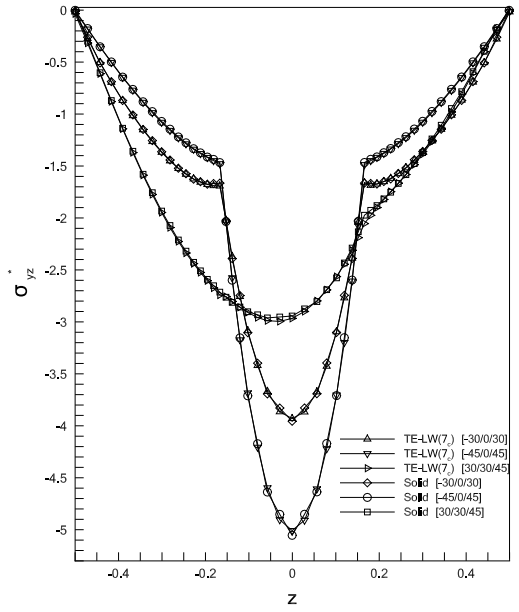

(c) σ^*_{yz} at y = L/2

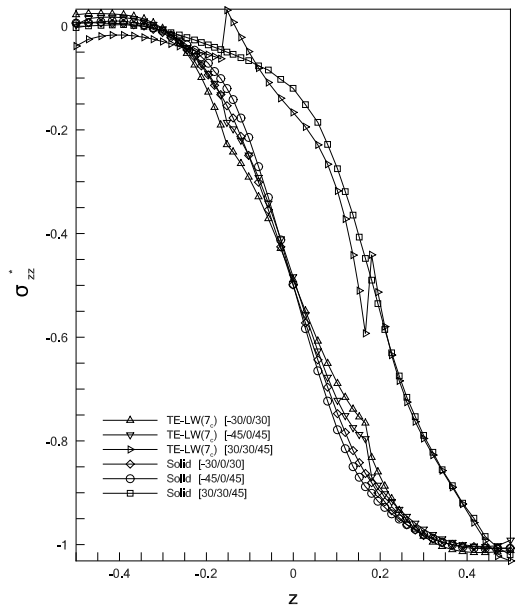

(d) σ^*_{zz} at y = L/2

Figure 9: Through-the-thickness distributions of stresses and transverse displacement of the 3-layer laminated beam $[\theta_1/\theta_2/\theta_3]$.

4.3 Sandwich beam with soft core

The considered cantilevered structure consisted of 3-layers of the same thickness and subjected to a uniform pressure. The bottom and top face sheets were made up of the orthotropic material defined in the previous section, whereas the core material was considered isotropic with the following properties

$$\frac{E_{Lface}}{E_{core}} = 2612.12 \quad \nu_{core} = 0.27$$

Figure 10 shows comparisons of various TE-LW expansions and a converged 3D FE solution in terms of axial (Fig. 10-a) and, transverse (Fig. 10-b) displacements, as well as normal (Fig. 10-c) and, shear (Fig. 10-d) transverse stresses.

As expected, at least a cubic local approximation is required in order to properly describe the deformation field of the structure. In fact, both the displacement and stress distributions computed with the TE-LW(3_c) model agree closely with the solid solution. However, owing to the significant transverse anisotropy of sandwich structures, the use of different kinematic assumptions would be expedient. The current approach enables the solution to be locally refined while the displacement continuity is preserved over all the interfaces and, at the same time, the number of DOF is reduced. In this context, Fig. 11 shows comparisons of the "full" TE-LW(7_c) model and the two variable kinematics theories, TE-LW(4-7-4) and TE-LW(5-7-5), in which the displacement fields of the face sheets have been approximated by fourth and fifth-order expansions, respectively.

Despite the lower number of DOFs, the reduced models have provided almost the same results as the complete kinematic field. In fact, only slight differences have been observed in the prediction of σ_{zz} at the interfaces.

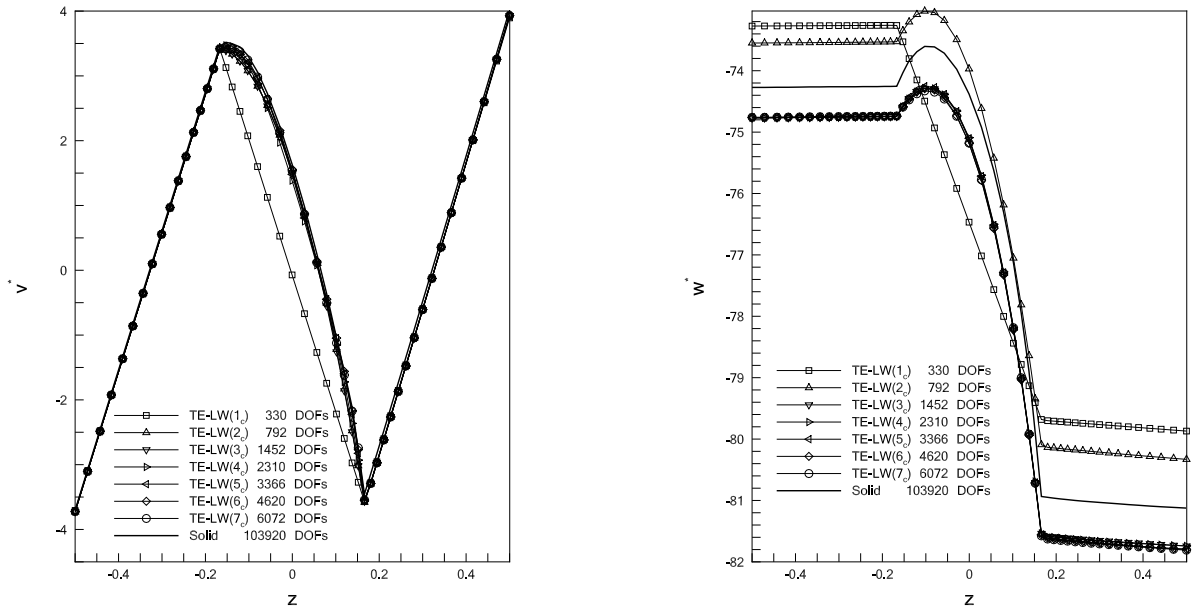

(a) v* at y = L

(b) w* at y = L

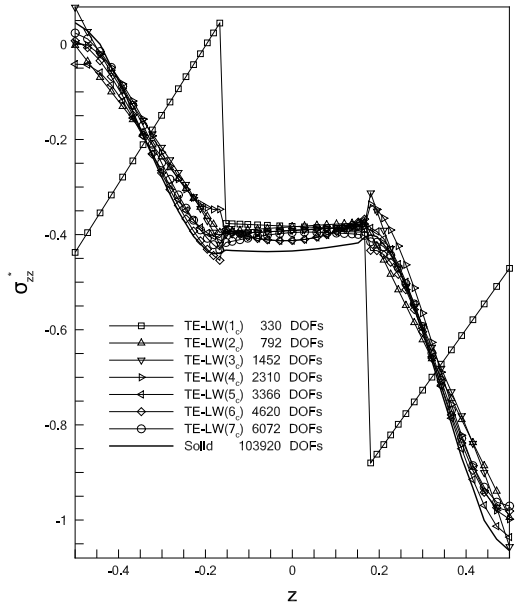

(c) σ^*_{zz} at y = L/2

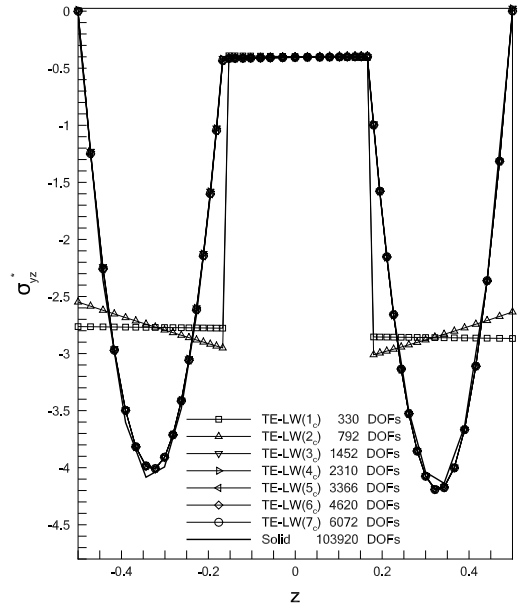

(d) σ^*_{yz} at y = L/2

Figure 10: Through-the-thickness distributions of displacements and stresses of the 3-layer sandwich beam [0/core/0].

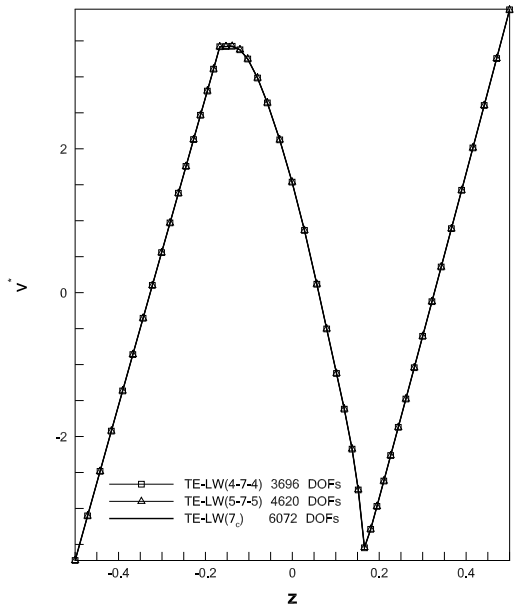

(a) v* at y = L

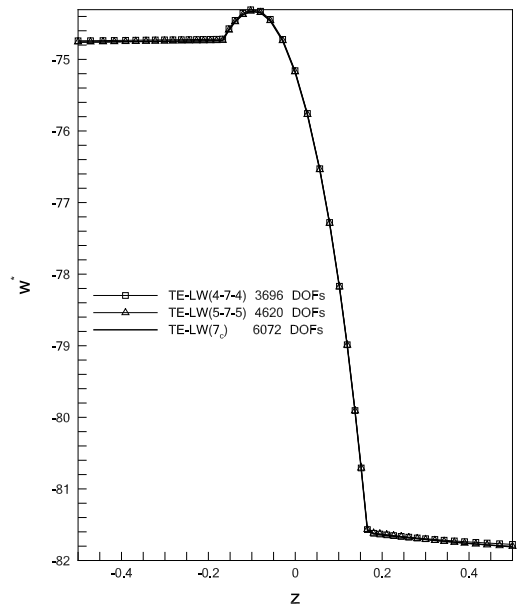

(b) w* at y = L

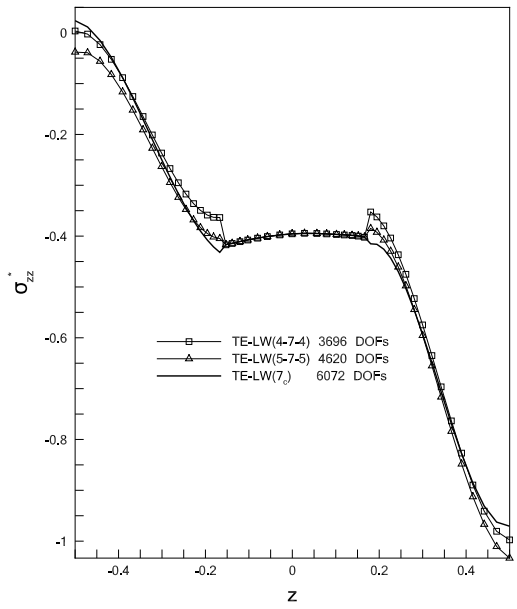

(c) σ^*_{zz} at y = L/2

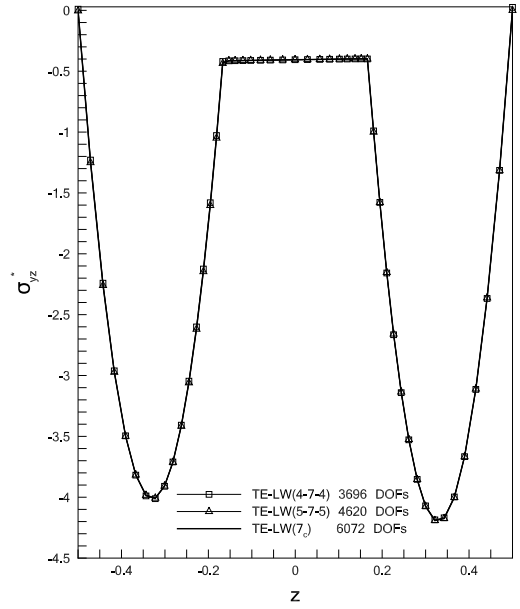

(d) σ^*_{yz} at y = L/2

Figure 11: Through-the-thickness distributions of displacements and stresses of the 3-layer sandwich beam [0/core/0].

5 Free-vibration analyses

The following section aims to present the results derived from the vibrational analyses of 1) antisymmetric [0/90] and symmetric [0/90/0] cross-ply laminated beams and 2) sandwich structures with a soft core. The aspect-ratio, L_s/b, of all the structures has been assumed equal to 5. The natural angular frequencies are expressed in the following dimensionless form

$$\bar{\omega} = \frac{L_s^2}{b}\sqrt{\frac{\rho}{E}}\,\omega \tag{11}$$

5.1 Cross-ply laminated beams

The square cross-section beams have been considered simply-supported and constituted of orthotropic material which has the following properties:

$$\frac{E_L}{E_T} = 25 \quad \frac{G_{LT}}{G_{TT}} = 2.5 \quad \nu_{LT} = \nu_{TT} = 0.25$$

The natural angular frequencies are reported in Tabs. 4-3 where, according to Eq. 11, Young's modulus is $E = E_T$. The results obtained by means of Navier-type [49] and finite element [30] solutions have been reported for comparison purposes. The considered mode shapes involve bending, torsional, shear and coupled deformations. Convergence has been achieved, for both lamination sequences, with the fourth-order expansion, which essentially provided the same results of the 3D solution. According to [30], the use of Murakami's zig-zag term determines significant improvements in the results with a negligible increase in the computational cost. It should be noted that the number of DOFs required for the proposed approach is comparable with that of zig-zag higher-order beam theories.

5.2 Sandwich beam with soft core

A sandwich beam consisting of structural face sheets (f) bonded to a core (c) has been considered; the parameters are

$$E_f = 200\,GPa \qquad E_c = 0.66\,GPa \qquad \nu_f = 0.3 \qquad \nu_c = 0.27$$

$$\rho_f = 7800\,Kg\,m^{-3}, \qquad \rho_c = 60\,Kg\,m^{-3}$$

The side dimension of the square cross-section and the thickness of face sheets have been assumed equal to $b = 0.02$ and $t_f = 0.003$ m, respectively. Simply-supported boundary conditions were applied at both ends. Tables 5 and 6 present the dimensionless frequency parameters (see Eq. 11, where the core density and Young's modulus are used) related to the modal shapes shown in Fig. 12. The current results have

	Mode I[a]	Mode II[b]	Mode III[c]	Mode IV[d]	Mode V[e]	DOFs
			Giunta *et al.* [49]			
FEM $3D_{20}$	4.9357	6.4491	9.0672	33.566	50.448	3843
TE23	4.9375	6.4603	9.0852	33.718	50.640	900
			Carrera *et al.* [30]			
EBBT	6.0083	10.102	-	57.186	-	198
FSDT	5.0738	7.5051	-	40.961	-	198
TE2	5.0551	6.9637	10.133	37.566	63.570	396
$TE2^{Mzz}$	5.0440	6.9632	10.133	36.384	59.734	462
TE3	4.9947	6.6601	9.8334	36.165	56.963	660
$TE3^{Mzz}$	4.9942	6.6593	9.8330	33.851	53.001	726
TE6	4.9462	6.5042	9.1550	34.153	51.527	1848
$TE6^{Mzz}$	4.9384	6.5037	9.1550	33.583	50.799	1914
			Present			
TE-LW(1_c)	5.0545	7.5248	10.237	33.908	62.116	264
TE-LW(2_c)	5.0194	6.8680	9.7713	33.625	55.885	594
TE-LW(3_c)	4.9363	6.4650	9.4585	33.571	52.381	1056
TE-LW(4_c)	4.9360	6.4549	9.0777	33.615	51.102	1650
TE-LW(5_c)	4.9359	6.4505	9.0739	33.587	50.664	2376

'-': mode not provided by the theory.

'Mzz': Murakami's zig-zag function.

[a] Flexural mode on plane yz.

[b] Flexural/torsional mode.

[c] Torsional mode.

[d] Axial/shear mode.

[e] Shear mode on plane xz.

Table 3: Dimensionless natural frequencies, L/b=5, [0/90] beam.

	Mode I[a]	Mode II[b]	Mode III[c]	Mode IV[d]	Mode V[e]	DOFs
			Giunta *et al.* [49]			
FEM $3D_{24}$	6.8888	7.4968	9.0386	55.536	57.912	5475
TE23	6.9252	7.5017	9.0683	55.914	58.135	900
			Carrera *et al.* [30]			
EBBT	13.752	11.552	-	-	64.722	198
FSDT	8.0853	8.0409	-	-	64.752	198
TE2	8.0837	8.0451	10.502	67.238	62.857	396
$TE2^{Mzz}$	7.0131	8.0451	10.502	66.319	62.893	462
TE3	7.1597	7.6230	10.502	59.912	62.824	660
$TE3^{Mzz}$	6.8990	7.6230	10.502	56.467	62.540	726
TE6	7.0610	7.5581	9.1952	57.429	59.315	1848
$TE6^{Mzz}$	6.8869	7.5581	9.1952	56.079	59.444	1914
TE8	6.9800	7.5279	9.1129	56.694	58.670	2970
$TE8^{Mzz}$	6.8886	7.5279	9.1129	55.729	58.886	3036
			Present			
TE-LW(1_c)	7.0144	8.0569	10.536	66.987	62.570	330
TE-LW(2_c)	6.9051	7.9665	9.5021	61.514	57.963	792
TE-LW(3_c)	6.8893	7.5042	9.4215	56.321	57.835	1452
TE-LW(4_c)	6.8891	7.5011	9.0508	56.020	57.934	2310
TE-LW(5_c)	6.8891	7.4980	9.0496	55.671	57.893	3366

'-': mode not provided by the theory.

'Mzz': Murakami's zig-zag function.

[a] Flexural mode on plane yz.

[b] Flexural mode on plane xy.

[c] Torsional mode.

[d] Shear mode on plane xz.

[e] Axial/shear mode.

Table 4: Dimensionless natural frequencies, L/b=5, [0/90/0] beam.

been compared with those presented in [50], where 1D Navier-type and 3D FE solutions were also used. As in the previous cases, the fourth-order TE-LW expansion provides an accurate description of the beam kinematics, except for the seventh mode shown in Tab. 6. In fact, it should be noted that the corresponding relative error, with respect to the 3D solution, is about 14%. This difference decreases to 1% when the TE-LW(5_c) theory, which essentially provides the same results as the 3D model, is used. Moreover, it has been observed that the frequencies related to the flexural modes in the yz plane (first columns of Tabs. 5 and 6) computed with TE-LW(2_c) are very close to the reference values.

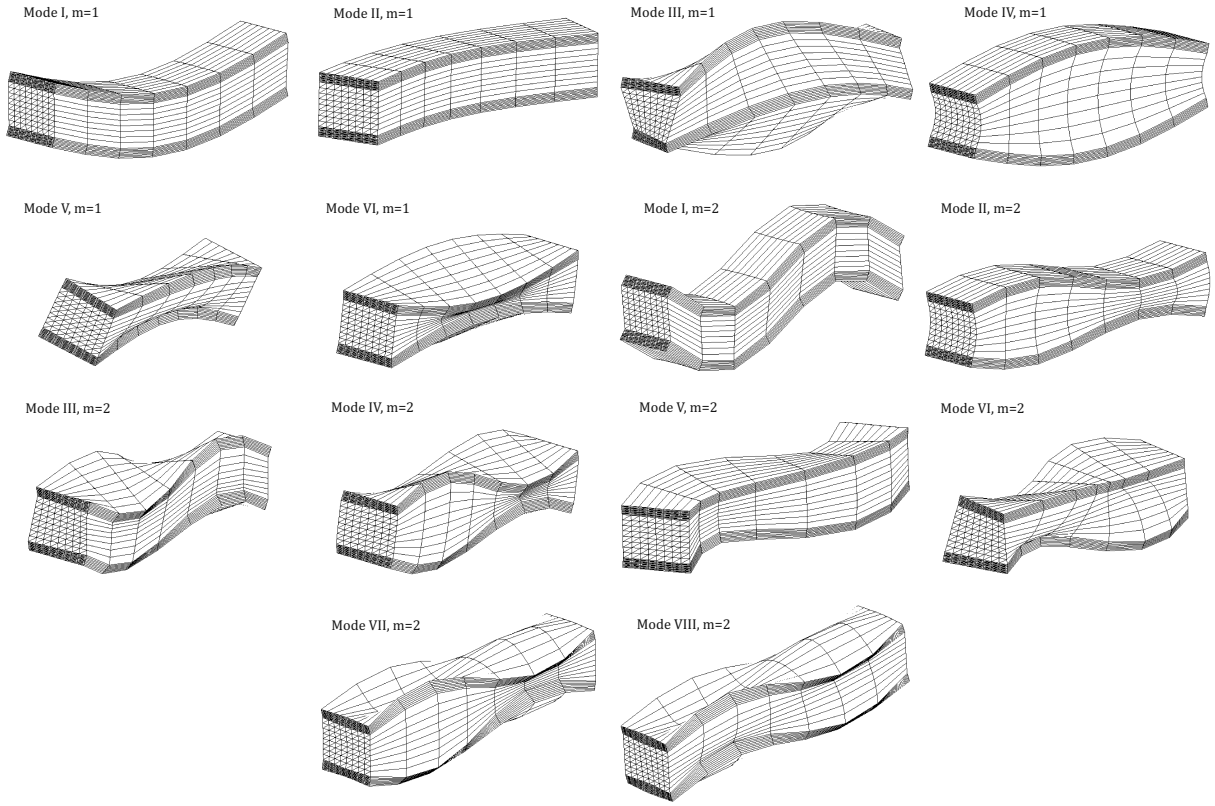

Figure 12: Mode shapes of the sandwich simply-supported beam.

Mode	I[a]	II[b]	III[c]	IV[d]	V[e]	VI[f]
			Giunta *et al.* [50]			
FEM 3D-a	1.097	2.669	2.920	6.641	6.670	7.092
TE19	1.142	2.669	2.953	6.997	7.055	7.482
TE15	1.154	2.669	2.967	7.096	7.175	7.635
TE8	1.245	2.669	3.018	7.840	8.276	8.144
			Present			
TE-LW(1_c)	1.124	3.073	9.719	6.980	11.89	-
TE-LW(2_c)	1.093	2.683	3.040	6.895	7.454	7.482
TE-LW(3_c)	1.092	2.668	2.962	6.646	6.982	7.467
TE-LW(4_c)	1.092	2.668	2.931	6.644	6.959	7.118
TE-LW(5_c)	1.092	2.668	2.931	6.628	6.709	7.113

'-': mode not provided by the theory.

[a] Flexural mode on plane yz.

[b] Flexural mode on plane xy.

[c] Torsional mode.

[d] Sheet face bending.

[e] Antisymmetric sheet faces twisting.

[e] Symmetric sheet faces twisting.

Table 5: Dimensionless natural frequencies, sandwich beam, $m = 1$.

Mode	I[a]	II[b]	III[c]	IV[d]	V[e]	VI[f]	VII[g]	VIII[h]
				Giunta *et al.* [50]				
FEM 3D-a	2.660	6.716	7.447	8.730	9.299	10.25	26.96	27.03
TE19	2.746	7.047	7.625	9.042	9.314	10.41	27.21	27.38
TE15	2.770	7.140	7.687	9.149	9.336	10.47	27.32	27.53
TE8	2.949	7.829	8.065	9.665	9.269	11.07	28.24	28.65
				Present				
TE-LW(1_c)	2.842	7.208	19.43	-	10.55	20.58	-	-
TE-LW(2_c)	2.663	6.911	7.988	9.181	9.464	10.96	-	36.13
TE-LW(3_c)	2.656	6.722	7.707	9.106	9.320	10.50	31.83	32.62
TE-LW(4_c)	2.654	6.718	7.590	8.806	9.298	10.37	30.75	27.73
TE-LW(5_c)	2.653	6.704	7.511	8.793	9.298	10.26	27.25	27.36

'-': mode not provided by the theory.

[a] Flexural mode on plane yz.

[b] Sheet faces bending.

[c] Torsional mode.

[d] Symmetric sheet faces twisting.

[e] Flexural mode on plane xy.

[f] Antisymmetric sheet faces twisting.

[g] Symmetric sheet face bending with through-the-width bending.

[h] Antisymmetric sheet face bending with through-the-width bending.

Table 6: Dimensionless natural frequencies, sandwich beam, $m = 2$.

6 Conclusions

This paper has evaluated the capabilities of a new class of displacement beam theories developed within the CUF framework. The Principle of Virtual Displacements has been used to derive the governing equations, which have been solved by means of the Finite Element method. Numerical simulations have been carried out on prismatic beams with rectangular cross-sections made of orthotropic and isotropic materials. Symmetric, antisymmetric and arbitrary stacking sequences have been considered. In the light of the results, the following conclusions can be drawn:

- the displacements and stress distributions computed with TE-LW theories agreed closely with the reference solutions, regardless of of which lamination was considered;
- accurate predictions of the shear stress distributions have been achieved, even though they were computed directly from Hooke's law;
- the higher-order TE-LW models essentially reproduced the same results, in terms of natural frequencies and mode shapes, as the 3D FE solutions, even for structures with high transverse degrees of anisotropy;
- this formulation is able to provide a valuable trade-off between computational cost and accuracy, since it has the flexibility to treat each subdomain independently;
- despite the encouraging results, the definition of the piecewise continuous functions can be difficult for complex-shaped cross-sections.

References

[1] L. Euler. *De curvis elasticis*. Bousquet, Geneva, 1744.

[2] S.P. Timoshenko and J.N. Goodier. *Theory of elasticity*. McGraw-Hill, New York, 1970.

[3] J.E. Ashton and J. M. Whitney. *Theory of laminated plates*, volume 4. CRC Press, 1970.

[4] E. Reissner. The effect of transverse shear deformation on the bending of elastic plates. 1945.

[5] K.H. Lo, R.M. Christensen, and E.M. Wu. A high-order theory of plate deformation, part 1: Homogeneous plates. *Journal of applied mechanics*, 44(4):663–668, 1977.

[6] K.H. Lo, R.M. Christensen, and E.M. Wu. A high-order theory of plate deformation, part 2: laminated plates. *Journal of Applied Mechanics*, 44(4):669–676, 1977.

[7] M.V.V. Murthy. An improved transverse shear deformation theory for laminated antisotropic plates. 1981.

[8] J.N. Reddy. A simple higher-order theory for laminated composite plates. *Journal of applied mechanics*, 51(4):745–752, 1984.

[9] Ozden O. Ochoa and J.N. Reddy. *Finite element analysis of composite laminates*. Springer, 1992.

[10] H. Matsunaga. Interlaminar stress analysis of laminated composite beams according to global higher-order deformation theories. *Composite Structures*, 55(1):105–114, 2002. doi: 10.1016/S0263-8223(01)00134-9.

[11] M. Touratier. An efficient standard plate theory. *International journal of engineering science*, 29(8):901–916, 1991.

[12] J.L. Mantari, A.S. Oktem, and C. Guedes Soares. A new trigonometric shear deformation theory for isotropic, laminated composite and sandwich plates. *International Journal of Solids and Structures*, 49(1):43–53, 2012.

[13] M. Karama, K.S. Afaq, and S. Mistou. A new theory for laminated composite plates. *Proceedings of the Institution of Mechanical Engineers, Part L: Journal of Materials Design and Applications*, 223(2):53–62, 2009.

[14] Maenghyo Cho and J-S Kim. Higher-order zig-zag theory for laminated composites with multiple delaminations. *Journal of Applied Mechanics*, 68(6):869–877, 2001.

[15] H. Arya, R.P. Shimpi, and N.K. Naik. A zigzag model for laminated composite beams. *Composite structures*, 56(1):21–24, 2002.

[16] Mihir K. Pandit, Abdul H. Sheikh, and Bhrigu N. Singh. An improved higher order zigzag theory for the static analysis of laminated sandwich plate with soft core. *Finite Elements in Analysis and Design*, 44(9):602–610, 2008.

[17] V.R. Aitharaju and R.C. Averill. C-0 zig-zag finite element for analysis of laminated composite beams. *Journal of Engineering mechanics*, 125(3):323–330, 1999.

[18] M.K. Rao and Y.M. Desai. Analytical solutions for vibrations of laminated and sandwich plates using mixed theory. *Composite Structures*, 63(3):361–373, 2004.

[19] A. Toledano and H. Murakami. A high-order laminated plate theory with improved in-plane responses. *International Journal of solids and Structures*, 23(1):111–131, 1987.

[20] E. Carrera. Historical review of zig-zag theories for multilayered plates and shells. *Applied mechanics reviews*, 56(3):287–308, 2003.

[21] M. Kameswara Rao, Y.M. Desai, and M.R. Chitnis. Free vibrations of laminated beams using mixed theory. *Composite Structures*, 52(2):149–160, 2001. doi: 10.1016/S0263-8223(00)00162-8.

[22] Chuijin Yang, Jubing Chen, and Shexu Zhao. The interlaminar stress of laminated composite under uniform axial deformation. *Modeling and Numerical Simulation of Material Science*, 3(02):49, 2013.

[23] R.P. Shimpi and Y.M. Ghugal. A new layerwise trigonometric shear deformation theory for two-layered cross-ply beams. *Composites Science and Technology*, 61(9):1271–1283, 2001. doi: 10.1016/S0266-3538(01)00024-0.

[24] R.P. Shimpi and A.V. Ainapure. A beam finite element based on layerwise trigonometric shear deformation theory. *Composite structures*, 53(2):153–162, 2001.

[25] E.J. Barbero and J.N. Reddy. Modeling of delamination in composite laminates using a layer-wise plate theory. *International Journal of Solids and Structures*, 28(3):373–388, 1991.

[26] Hossein Hosseini-Toudeshky, Samira Hosseini, and Bijan Mohammadi. Delamination buckling growth in laminated composites using layerwise-interface element. *Composite Structures*, 92(8):1846–1856, 2010.

[27] M.L. Liu and J. Yu. Finite element modeling of delamination by layerwise shell element allowing for interlaminar displacements. *Composites science and technology*, 63(3):517–529, 2003.

[28] G Giunta, S Belouettar, H Nasser, EH Kiefer-Kamal, and T Thielen. Hierarchical models for the static analysis of three-dimensional sandwich beam structures. *Composite Structures*, 133:1284–1301, 2015.

[29] E. Carrera, M. Filippi, and E. Zappino. Laminated beam analysis by polynomial, trigonometric, exponential and zig-zag theories. *European Journal of Mechanics - A/Solids*, 41(0):58 – 69, 2013. doi: 10.1016/j.euromechsol.2013.02.006.

[30] E. Carrera, M. Filippi, and E. Zappino. Free vibration analysis of laminated beam by polynomial, trigonometric, exponential and zig-zag theories. *Journal of Composite Materials*, 2013. doi: 10.1177/0021998313497775.

[31] M. Filippi, E. Carrera, and A.M. Zenkour. Static analyses of fgm beams by various theories and finite elements. *Composites Part B: Engineering*, 72:1–9, 2015.

[32] Daoud S. Mashat, E. Carrera, Ashraf M. Zenkour, Sadah A. Al Khateeb, and M Filippi. Free vibration of fgm layered beams by various theories and finite elements. *Composites Part B: Engineering*, 59:269–278, 2014.

[33] E. Carrera, M. Filippi, P.K.R. Mahato, and A. Pagani. Advanced models for free vibration analysis of laminated beams with compact and thin-walled open/closed sections. *Journal of Composite Materials*, 2014. doi: 10.1177/0021998314541570.

[34] E. Carrera, M. Filippi, P.K. Mahato, and A. Pagani. Accurate static response of single-and multi-cell laminated box beams. *Composite Structures*, 136:372–383, 2016.

[35] A. Pagani, A.G. de Miguel, M. Petrolo, and E. Carrera. Analysis of laminated beams via unified formulation and legendre polynomial expansions. *Composite Structures*, 2016.

[36] E. Carrera and A. Pagani. Multi-line enhanced beam model for the analysis of laminated composite structures. *Composites Part B: Engineering*, 57:112–119, 2014.

[37] Jie Yang, Qun Huang, Heng Hu, Gaetano Giunta, Salim Belouettar, and Michel Potier-Ferry. A new family of finite elements for wrinkling analysis of thin films on compliant substrates. *Composite Structures*, 119:568–577, 2015.

[38] M. Botshekanan Dehkordi, M. Cinefra, S.M.R. Khalili, and E. Carrera. Mixed lw/esl models for the analysis of sandwich plates with composite faces. *Composite Structures*, 98:330–339, 2013.

[39] A. Pagani, S. Valvano, and E. Carrera. Analysis of laminated composites and sandwich structures by variable-kinematic mitc9 plate elements. *Journal of Sandwich Structures and Materials*, 2016. In press.

[40] M Botshekanan Dehkordi, SMR Khalili, and E Carrera. Non-linear transient dynamic analysis of sandwich plate with composite face-sheets embedded with shape memory alloy wires and flexible core-based on the mixed lw (layer-wise)/esl (equivalent single layer) models. *Composites Part B: Engineering*, 87:59–74, 2016.

[41] E. Carrera, G. Giunta, and M. Petrolo. *Beam Structures Classical and Advanced Theories*. John Wiley & Sons, Ltd, The Atrium, Southern Gate, Chichester, West Sussex, PO19 8SQ, United Kingdom, 2011.

[42] E. Carrera and M. Filippi. Variable kinematic one-dimensional finite elements for the analysis of rotors made of composite materials. *Journal of Engineering for Gas Turbines and Power*, 136(9):092501, 2014.

[43] E. Carrera, M. Cinefra, M. Petrolo, and E. Zappino. *Finite Element Analysis of Structures through Unified Formulation*. John Wiley & Sons Ltd, 2014.

[44] Sergei Georgievich Lekhnitskii. Anisotropic plates. Technical report, DTIC Document, 1968.

[45] K.S. Surana and S.H. Nguyen. Two-dimensional curved beam element with higher-order hierarchical transverse approximation for laminated composites. *Computers and Structures*, 36(3):499–511, 1990. doi: 10.1016/0045-7949(90)90284-9.

[46] J.F. Davalos, Y. Kim, and E.J. Barbero. Analysis of laminated beams with a layer-wise constant shear theory. *Composite Structures*, 28(3):241 – 253, 1994.

[47] X. Lin and Y.X. Zhang. A novel one-dimensional two-node shear-flexible layered composite beam element. *Finite Elements in Analysis and Design*, 47(7):676 – 682, 2011. doi: 10.1016/j.finel.2011.01.010.

[48] T.P. Vo and H. Thai. Static behavior of composite beams using various refined shear deformation theories. *Composite Structures*, 94(8):2513 – 2522, 2012. doi: 10.1016/j.compstruct.2012.02.010.

[49] G. Giunta, F. Biscani, S. Belouettar, A.J.M. Ferreira, and E. Carrera. Free vibration analysis of composite beams via refined theories. *Composites Part B: Engineering*, 44(1):540–552, 2013.

[50] G. Giunta, N. Metla, Y. Koutsawa, and S. Belouettar. Free vibration and stability analysis of three-dimensional sandwich beams via hierarchical models. *Composites Part B: Engineering*, 47:326–338, 2013.